



# A new Google Earth Engine tool for spaceborne detection of buried palaeogeographical features – examples from the Nile Delta (Egypt)

Tobias Ullmann<sup>1,2</sup>, Eric Möller<sup>2</sup>, Roland Baumhauer<sup>2</sup>, Eva Lange-Athinodorou<sup>3</sup>, and Julia Meister<sup>2</sup>

<sup>1</sup>Remote Sensing, Institute of Geography and Geology, University of Würzburg, 97074 Würzburg, Germany

<sup>2</sup>Physical Geography, Institute of Geography and Geology, University of Würzburg, 97074 Würzburg, Germany

<sup>3</sup>Institute of Egyptology, University of Würzburg, 97070 Würzburg, Germany

**Correspondence:** Tobias Ullmann ([tobias.ullmann@uni-wuerzburg.de](mailto:tobias.ullmann@uni-wuerzburg.de))  
and Julia Meister ([julia.meister@uni-wuerzburg.de](mailto:julia.meister@uni-wuerzburg.de))

**Relevant dates:** Received: 27 July 2022 – Revised: 12 October 2022 – Accepted: 27 October 2022 –  
Published: 18 November 2022

**How to cite:** Ullmann, T., Möller, E., Baumhauer, R., Lange-Athinodorou, E., and Meister, J.: A new Google Earth Engine tool for spaceborne detection of buried palaeogeographical features – examples from the Nile Delta (Egypt), *E&G Quaternary Sci. J.*, 71, 243–247, <https://doi.org/10.5194/egqsj-71-243-2022>, 2022.

## 1 Introduction

With the opening of the Landsat archive in 2002, the largest remote sensing archive became available to the public (Wulder et al., 2012). This record presents the most comprehensive civil database on the Earth's surface, and it has stimulated research across the globe for many disciplines (Wulder et al., 2016). Several spaceborne remote sensing missions have since then been launched (Belward and Skøien, 2015), some of them operating now for more than 20 years, such as the highly successful missions carrying the MODIS instrument. Furthermore, recent spaceborne earth observation missions not only continue the building of global remote sensing archives using various sensors but also significantly increased the temporal and spatial resolution (e.g. the Sentinel-2 mission), allowing the dynamics of the Earth to be studied at so far unprecedented spatio-temporal resolution on a global scale. These datasets have also contributed to the field of geomorphology and geoarchaeology. Exemplarily, Brandolini et al. (2021) and Orenco and Petrie (2017) used time series of the Sentinel-2 or Landsat mission to infer and map differences in soil and moisture properties re-

lated to historic or palaeogeographical features. Further, Ullmann et al. (2020) have investigated long-term differences in the normalized difference water index (NDWI) in the Nile Delta to map buried palaeogeographical features, i.e. related to former river branches of the Nile, or buried Pleistocene sand hills (“geziras”) often used as settlement mounts. While these archives and datasets certainly offer new opportunities, the handling and analyses come with challenges, most strikingly arising from the enormous data load and the high computing effort. Fortunately, some of these limitations can be overcome by recently available cloud-computing capacities, exemplarily offered by the Google Earth Engine (GEE) (Gorelick et al., 2017). These capacities allow processing and analysing large stacks of earth observation data in a cloud environment in a very fast and efficient manner without the need of downloading and processing the raw data. To make these new developments applicable for users with less experience in remote sensing, we present here a freely available GEE tool that allows the processing of remote sensing archive data from Landsat, MODIS, and Sentinel-2 in a user-friendly way. The tool is based on the GEE efforts of previ-

ous research (Ullmann et al., 2020) but provides an improved and ready-to-use browser-based application that is suitable for users who are less familiar with GEE. In this contribution, we exemplarily show the processing results of the tool for the entire Nile Delta for Landsat, MODIS, and Sentinel-2 and continue mapping buried palaeogeographical features using the long-term differences in NDWI (see Ullmann et al., 2020).

## 2 Study area

The Egyptian Nile Delta covers about 24 000 km<sup>2</sup> and is the largest delta of the Mediterranean Sea. Historic textual sources witness up to seven major Nile branches that flowed through the delta, while today only the Rosetta and Damietta branches exist (Fig. 1; Bietak, 1975). In antiquity, these waterways were of high significance for intra-Egyptian trade and traffic, and major ancient Egyptian cities are exclusively found in their immediate surroundings. Hence, the reconstruction of the Holocene delta environments is also crucial for studying the human–environment interactions of ancient Egypt (Butzer, 1976; Pennington et al., 2017; Bietak, 1975). For protection against the seasonal Nile floods, settlements were either built on Pleistocene sand mounds (“geziras”) or on the embankments of the river branches. However, due to the long-term dynamics of the riverine system, the landscape of the Nile Delta has constantly changed. Water courses have been silted up and are no longer visible in the modern landscape. Knowing about the importance of localizing the route of former Nile branches, several geophysical and geoarchaeological investigations were carried out in the past, of which some also rely on remotely sensed imagery, e.g. Ginou et al. (2017) and El-Fadaly et al. (2019).

## 3 Material and methods

In continuation of these efforts, the processing of remote sensing time series of Landsat (including Landsat 9 and Collection 2 data), Sentinel-2 and MODIS was conducted using the cloud-based processing capacities of the GEE. For this purpose, we developed a script which allows the generation of cloud-free surface reflectance products and various spectral indices for a user-defined period, region of interest, and for the earth observation data of the respective sensors. The source code of this tool is freely available on GitHub ([https://github.com/EricMoeller96/master\\_thesis](https://github.com/EricMoeller96/master_thesis), last access: 9 November 2022) and comes with documentation on the most important settings. The tool requires a minimum of user inputs for the execution and can be executed for a user-defined region. Exemplarily, the datasets, specified in Table 1, were processed to generate median RGB composites for the entire Nile Delta (Fig. 1). In addition, multispectral indices, such as the normalized difference vegetation index (NDVI), NDWI (Gao, 1996), and normalized difference

snow index (NDSI), are calculated and processed by default. Following the approach presented in a preceding work (Ullmann et al., 2020), in this study we exemplarily focus on two median NDWI images which were calculated from the time series: one for the winter (January/February) and one for the summer (July/August) seasons and for each sensor. These NDWI images were then differenced (summer minus winter) to draw the long-term seasonal difference ( $\Delta$ NDWI; Fig. 2).

## 4 First results and discussion

The GEE script allows cloud-free summer and winter mosaics to be processed for the entire Nile Delta in a fast manner and for all sensors (Fig. 1) using analysis-ready products (i.e. surface reflectance). Processing time in the GEE was about 10 to 30 min, which would not be achievable using standard computing facilities given the high number of scenes (e.g. more than 1900 scenes for Landsat).

Thus, the analyses are not limited to the spectral indices, but the multispectral information can also be utilized, which opens possibilities for further investigations apart from the differentiation of spectral indices, e.g. time series analysis or land cover classification. The  $\Delta$ NDWI images of all three sensors show corresponding positive and negative anomalies on the broadest scale (Fig. 2), which follow the general systematic outlined in Ullmann et al. (2020). As such, the largest and strongest anomalies likely display distinctive features of the general (palaeo-)environmental setting as sketched by Butzer (1976). For instance, strong negative anomalies of the  $\Delta$ NDWI somewhat match the proposed location of sands at or near the surface at several locations between the modern course of the Rosetta and the Damietta branches and between Tanta and Cairo. In all datasets negative  $\Delta$ NDWI values are found in the western Nile Delta (south of Alexandria and west of Damanhur), the central Nile Delta (south of Tanta towards Cairo), and in the northern Nile Delta (in the vicinity of Lake Burullus). Positive  $\Delta$ NDWI values are less frequent, and the largest patches are found near Lake Burullus (north) and Lake Manzala (east). Obviously, the higher spatial resolution of Landsat and Sentinel-2 allows a more detailed picture to be depicted; in both datasets spatially varying positive and negative anomalies are found in the delta west of the Rosetta branch. Overall, Sentinel-2 data deliver a better geometric resolution revealing more details (e.g. as exemplified for Geziret Sineita in Fig. 2d–f); however, due to the rather short time series of 4 years (compared to 36 years offered by Landsat), anomalies are less clear, and the  $\Delta$ NDWI image shows more heterogeneities compared to the results of Landsat. This is also displayed by the higher deviation used to scale the  $\Delta$ NDWI images (Fig. 2). It is likely that this issue is linked to the short time series as seasonal differences in NDWI become best visible when long timescales are analysed (Ullmann et al., 2020). As such, a long observation

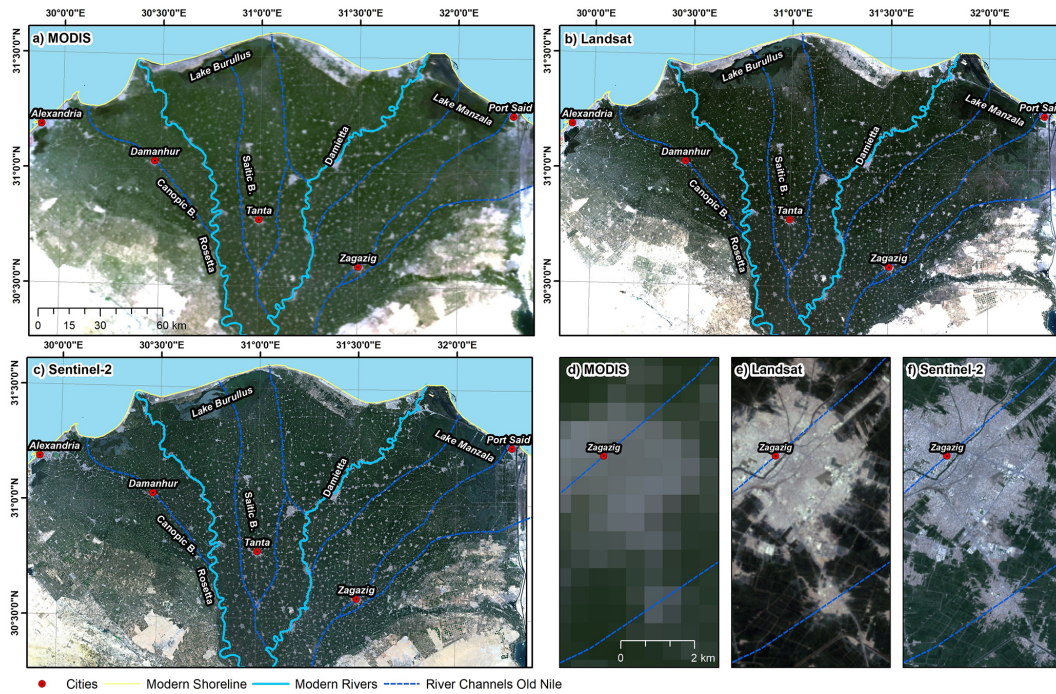


**Figure 1.** Comparison of cloud-free summer (July/August) median RGB composites of the Nile Delta: (a) MODIS (2001–2021), (b) Landsat (1985–2021), (c) Sentinel-2 (2017–2021), and (d–f) detailed views of the city of Zagazig. Ancient river channels of the Nile are drawn according to Pennington et al. (2017).

**Table 1.** Overview of investigated remote sensing datasets which were processed using the Google Earth Engine. Bands refer to B = blue, G = green, R = red, NIR = near infrared, and SWIR = short-wave infrared. Multispectral indices and products are as follows: NDVI = normalized difference vegetation index, NDWI = normalized difference water index, NDSI = normalized difference snow index, NBR = normalized burn ratio, and LST = land surface temperature. Composites of each band, index, and product were generated using the median operator; as such, a pixel shows the median value over the entire stack of all cloud-free acquisitions within the period of investigation.

Mission	Resampled geometric resolution (m)	Bands	Multispectral indices and products	Period of investigation	Number of images
MODIS	500	B, G, R, NIR1, NIR2, SWIR1, SWIR2	NDVI, NDWI, NBR, NDSI, LST	January/February 2001 to 2021	1240
MODIS	500	B, G, R, NIR1, NIR2, SWIR1, SWIR2	NDVI, NDWI, NBR, NDSI, LST	July/August 2001 to 2021	1363
Landsat	30	B, G, R, NIR, SWIR1, SWIR2	NDVI, NDWI, NBR, NDSI	January/February 1985 to 2021	620
Landsat	30	B, G, R, NIR, SWIR1, SWIR2	NDVI, NDWI, NBR, NDSI	July/August 1985 to 2021	1310
Sentinel-2	20	B, G, R, Red Edge 1, Red Edge 2, Red Edge 3, NIR, Red Edge 4, SWIR1, SWIR2	NDVI, NDWI, NBR, NDSI	January/February 2017 to 2021	412
Sentinel-2	20	B, G, R, Red Edge 1, Red Edge 2, Red Edge 3, NIR, Red Edge 4, SWIR1, SWIR2	NDVI, NDWI, NBR, NDSI	July/August 2017 to 2021	814

period is important to identify rather weak anomalies in the  $\Delta$ NDWI. Thus for now, the Landsat archive appears to be the most useful and promising record for identifying  $\Delta$ NDWI anomalies associated with surface and near-surface discontinuities in soil properties. Taking this further, Fig. 3 shows

preliminary results from the continued mapping efforts. The visual analysis of the Landsat  $\Delta$ NDWI revealed several additional linear and meandering anomalies, especially between Damanhur and Tanta and in the surroundings of Zagazig. Some of them correspond remarkably well with the general

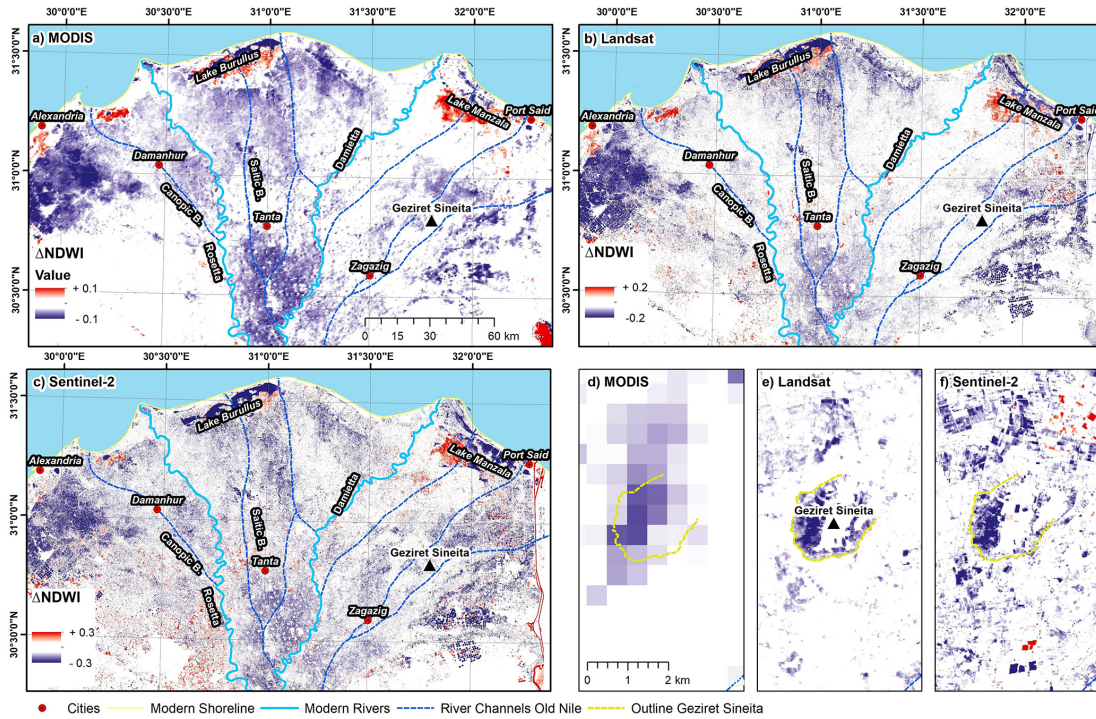


**Figure 2.** Comparison of  $\Delta$ NDWI anomalies of the Nile Delta: (a) MODIS (2001–2021), (b) Landsat (1985–2021), (c) Sentinel-2 (2017–2021), and (d–f) detailed views of Geziret Sineita (Tell es-Sunayta) (see van den Brink, 1987). Ancient river channels of the Nile are drawn according to Pennington et al. (2017).

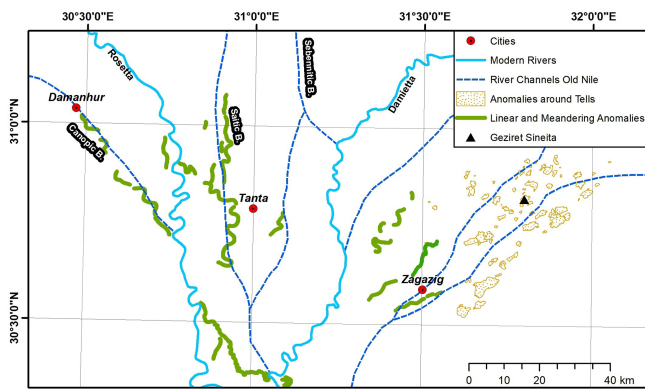


**Figure 3.** Preliminary mapping results of  $\Delta$ NDWI anomalies in the central Nile Delta based on Landsat imagery (1985–2021). Ancient river channels of the Nile are drawn according to Pennington et al. (2017).

flow directions and river routes indicated by Pennington et al. (2017). These anomalies could therefore indicate former courses of the Canopic Branch and Saitic Branch.

**5 Conclusion**

The increased number and availability of spaceborne remote sensing records, their enhanced spatio-temporal resolution,

and latest cloud-based processing capacities open new opportunities to study the nature and dynamics of the land surface on a local to global scale. This opens opportunities in the field of geomorphology and geoarchaeology, e.g. in the context of landscape archaeology. In the present contribution, we highlight as an example the application of a freely available Google Earth Engine (GEE) tool to process cloud-free composites for the Nile Delta using the archives of MODIS, Landsat, and Sentinel-2. Following a preliminary approach, seasonal differences in the NDWI were investigated and interpreted in the context of buried palaeogeographical features. Among the investigated data, the Landsat archive offers the most promising record to identify spectral anomalies related to surface and surficial discontinuities of soil and land properties. Given the global availability of remote sensing data from Sentinel-2, Landsat, and MODIS, as well as the capacities that arise from the Google Earth Engine, a transfer to other sites with similar environmental conditions (e.g. continuous rather than homogeneous land cover) seems certainly feasible and of interest for future investigations.

**Code and data availability.** Data relating to this paper are available from the corresponding authors upon reasonable request. The Google Earth Engine code is available at <https://doi.org/10.5281/zenodo.7313130> (EricMoeller96, 2022).

**Author contributions.** The methodology was developed by TU and EM. The formal analysis was conducted by TU and EM. TU, EM, RB, ELA and JM interpreted the results jointly. Funding was acquired by TU and JM. The manuscript was prepared by TU and JM with contributions from all authors.

**Competing interests.** At least one of the (co-)authors is a member of the editorial board of *E&G Quaternary Science Journal*. The peer-review process was guided by an independent editor, and the authors also have no other competing interests to declare.

**Disclaimer.** Publisher's note: Copernicus Publications remains neutral with regard to jurisdictional claims in published maps and institutional affiliations.

**Special issue statement.** This article is part of the special issue "Quaternary research from and inspired by the first virtual DEUQUA conference". It is a result of the vDEUQUA2021 online conference in September/October 2021.

**Acknowledgements.** We are grateful to Janek Walk for providing valuable feedback.

**Financial support.** This research has been supported by the Deutsche Forschungsgemeinschaft (DFG, German Research Foundation; grant no. 507687060).

This open-access publication was funded by Julius-Maximilians-Universität Würzburg.

**Review statement.** This paper was edited by Christian Zeeden and reviewed by Janek Walk.

## References

Belward, A. S. and Skoien, J. O.: Who launched what, when and why; trends in global land-cover observation capacity from civilian earth observation satellites, *ISPRS J. Photogramm.*, 103, 115–128, <https://doi.org/10.1016/j.isprsjprs.2014.03.009>, 2015.

Bietak, M.: Tell El-Dab'a II: Der Fundort im Rahmen einer archäologisch-geographischen Untersuchung über das ägyptische Ostdelta, in: *Untersuchungen der Zweigstelle Kairo des Österreichischen Archäologischen Instituts*, Verlag der Österreichischen Akademie der Wissenschaften, Wien, 236 pp., ISBN 978-3-7001-0136-9, 1975.

Brandolini, F., Domingo-Ribas, G., Zerboni, A., and Turner, S.: A Google Earth Engine-enabled Python approach for the identification of anthropogenic palaeo-landscape features, *Open Res Europe*, 1, 22, <https://doi.org/10.12688/openreseurope.13135.2>, 2021.

Butzer, K. W.: *Early hydraulic civilization in Egypt: a study in cultural ecology*, University of Chicago Press, Chicago, 134 pp., ISBN: 0-226-08634-8, 1976.

El-Fadaly, A., Abouarab, M. A. R., El Shabrawy, R. R. M., Mostafa, W., Wilson, P., Morhange, C., Silverstein, J., and Lasaponara, R.: Discovering Potential Settlement Areas around Archaeological Tells Using the Integration between Historic Topographic Maps, Optical, and Radar Data in the Northern Nile Delta, Egypt, *Remote Sens.*, 11, 3039, <https://doi.org/10.3390/rs11243039>, 2019.

EricMoeller96: EricMoeller96/master\_thesis: Script\_by\_Eric\_Moeller\_v6, Version V6, Zenodo [code], <https://doi.org/10.5281/zenodo.7313130>, 2022.

Gao, B.: NDWI–A normalized difference water index for remote sensing of vegetation liquid water from space, *Remote Sens. Environ.*, 58, 257–266, [https://doi.org/10.1016/S0034-4257\(96\)00067-3](https://doi.org/10.1016/S0034-4257(96)00067-3), 1996.

Ginau, A., Schiestl, R., Kern, F., and Wunderlich, J.: Identification of historic landscape features and settlement mounds in the Western Nile Delta by means of remote sensing time series analysis and the evaluation of vegetation characteristics, *Journal of Archaeological Science: Reports*, 16, 170–184, <https://doi.org/10.1016/j.jasrep.2017.09.034>, 2017.

Gorelick, N., Hancher, M., Dixon, M., Ilyushchenko, S., Thau, D., and Moore, R.: Google Earth Engine: Planetary-scale geospatial analysis for everyone, *Remote Sens. Environ.*, 202, 18–27, <https://doi.org/10.1016/j.rse.2017.06.031>, 2017.

Orengo, H. and Petrie, C.: Large-Scale, Multi-Temporal Remote Sensing of Palaeo-River Networks: A Case Study from Northwest India and its Implications for the Indus Civilisation, *Remote Sens.*, 9, 735, <https://doi.org/10.3390/rs9070735>, 2017.

Pennington, B. T., Sturt, F., Wilson, P., Rowland, J., and Brown, A. G.: The fluvial evolution of the Holocene Nile Delta, *Quaternary Sci. Rev.*, 170, 212–231, <https://doi.org/10.1016/j.quascirev.2017.06.017>, 2017.

Ullmann, T., Nill, L., Schiestl, R., Trappe, J., Lange-Athinodorou, E., Baumhauer, R., and Meister, J.: Mapping buried palaeogeographical features of the Nile Delta (Egypt) using the Landsat archive, *E&G Quaternary Sci. J.*, 69, 225–245, <https://doi.org/10.5194/egqsj-69-225-2020>, 2020.

van den Brink, E. C. M.: A Geo-Archaeological Survey in the North-Eastern Nile Delta, Egypt; the First Two Seasons, a Preliminary Report, *Mitteilungen des Deutschen Archäologischen Instituts, Abteilung Kairo*, 43, 7–31, 1987.

Wulder, M. A., Masek, J. G., Cohen, W. B., Loveland, T. R., and Woodcock, C. E.: Opening the archive: How free data has enabled the science and monitoring promise of Landsat, *Remote Sens. Environ.*, 122, 2–10, <https://doi.org/10.1016/j.rse.2012.01.010>, 2012.

Wulder, M. A., White, J. C., Loveland, T. R., Woodcock, C. E., Belward, A. S., Cohen, W. B., Fosnight, E. A., Shaw, J., Masek, J. G., and Roy, D. P.: The global Landsat archive: Status, consolidation, and direction, *Remote Sens. Environ.*, 185, 271–283, <https://doi.org/10.1016/j.rse.2015.11.032>, 2016.